1995

A Parallel-Plate Electrochemical Reactor Model for the Destruction of Nitrate and Nitrite in Alkaline Waste Solutions

D. H. Coleman
University of South Carolina - Columbia

Ralph E. White
University of South Carolina - Columbia, white@cec.sc.edu

D. T. Hobbs

Publication Info

Journal of the Electrochemical Society, 1995, pages 1152-1161.

10. G. Bourghesani and F. Pulidori, *Electrochim. Acta*, **29**, 107 (1984).
11. B. B. Damaskin and A. N. Frumkin, *J. Electroanal. Chem.*, **74**, 191 (1972).
12. G. M. Barrow, *Physical Chemistry*, McGraw-Hill Book Company, Inc., New York (1966).
13. K. Kondo, J. Ishikawa, O. Takenaka, T. Matsubara, and M. Irie, *This Journal*, **138**, 3629 (1991).

A Parallel-Plate Electrochemical Reactor Model for the Destruction of Nitrate and Nitrite in Alkaline Waste Solutions

D. H. Coleman* and R. E. White**

Department of Chemical Engineering, University of South Carolina, Columbia, South Carolina 29208

D. T. Hobbs**

Westinghouse Savannah River Company, Aiken, South Carolina 29808

ABSTRACT

A parallel-plate electrochemical reactor model with multiple reactions at both electrodes and anolyte and catholyte recirculation tanks was modeled for the electrochemical destruction of nitrate and nitrite species in an alkaline solution. The model can be used to predict electrochemical reaction current efficiencies and outlet concentrations of species from the reactor, given inlet feed conditions and cell operating conditions. Also, predictions are made for off-gas composition and liquid-phase composition in the recirculation tanks. The results of case studies at different applied potentials are shown here. At lower applied potentials, the model predictions show that the destruction process is more energy efficient, but the time required to destroy a given amount of waste is increased.

The electrochemical treatment of nuclear waste is the subject of much current interest. After radioactive decontamination, the liquid waste from nuclear fuel processing still contains many hazardous substances, among them nitrate and nitrite. Electrochemical reduction of the nitrate and nitrite destroys these hazardous species while simultaneously reducing the volume of the waste. The electrochemical reduction process has been shown to be an effective treatment in regard to the removal of nitrate and nitrite from simulated and real waste solutions, but further optimization of the process is still needed.[1,2]

No modeling of the parallel-plate electrochemical reactor has yet been done for a nitrate waste system. However, parallel-plate reactor models have been published for other systems. White *et al.*[3] presented a complete parallel-plate reactor model that was used to model multiple electrode reactions at the cathode. With this model for the electrowinning of copper, they were able to predict current efficiencies, selectivity, and conversion per pass for different reactor designs. However, they did not include multiple reactions at both electrodes nor a separator in their model. In addition no gas evolving reactions were modeled.

Mader *et al.*[4] made a simplification for the parallel-plate reactor model that substantially reduced the required computing time. They assumed that the change in concentration of a species with respect to reactor length could be approximated by a step change in concentration from the reactor inlet to the reactor outlet. This essentially changed the model from a two-dimensional model to a one-dimensional model. The new model was called the one-step model, and the old model was called the continuous model.

Mader and White[5] also developed a model for a Zn/Br_2 flow battery on charge. This model was similar to the others developed before[3,4] but included a separator region between the electrodes. Only the charge mode of the cell was modeled. The MacMullin number,[6] N_M, was used along with the separator thickness to describe the transport properties of the separator. Evans and White[7] later developed a model for both the discharging and charging modes of the Zn/Br_2 flow battery.

* Electrochemical Society Student Member.
** Electrochemical Society Active Member.

No parallel-plate reactor model of the type mentioned above includes the effect of gas evolution at the electrodes. Since most of the reactions in the nitrate waste system have gaseous products, this is an important area for investigation while constructing a model for this system. In general, gas evolution affects the ohmic resistance of cells, the mixing history of the solution, and mass transfer to and from the electrodes.[8] If the rate of gas evolution is small compared to the flow rate of the liquid phase, then the gas bubbles may not have a profound effect on the mixing in the reactor. Some experimental evidence was found for this case for an axially dispersed plug flow model.[8] According to Wu *et al.*,[8] at N_{Re} greater than 100, dispersion rates were not substantially affected by gas evolution. In addition, the mean residence time of Cu^+ ions was not substantially affected, even at low Reynolds numbers, by the presence of gas. Consequently, it is assumed in this work the gas evolution at the electrodes does not affect substantially the operating characteristics of the cell. It may be necessary in the future to add gas evolution effects at the electrodes for cases with small Reynolds numbers.

Several models for a parallel-plate electrochemical reactor with recirculation have been developed.[9-13] Most of the models assumed that the electrochemical reactor was in plug flow and did not consider the effect of potential, electrode gap, ionic migration, or electrode kinetics. Nguyen *et al.*[13] presented a two-dimensional model for a parallel-plate electrochemical reactor with a continuously stirred tank reactor (CSTR) and recirculation. The electrochemical reactor was similar to that developed by others[3-5,7] and included dependence on kinetics, applied potential, migration, and flow distribution. The model included time dependence in both the electrochemical reactor and the CSTR. Only one reaction at each electrode was modeled and one reaction in the reservoir. No separator was included in the model.

No model was found that included equilibrium between a liquid and gas phase. Nor have any of the models with recirculation tanks or CSTRs included a separator in the model. Both of these aspects are important in this research and are included in this work.

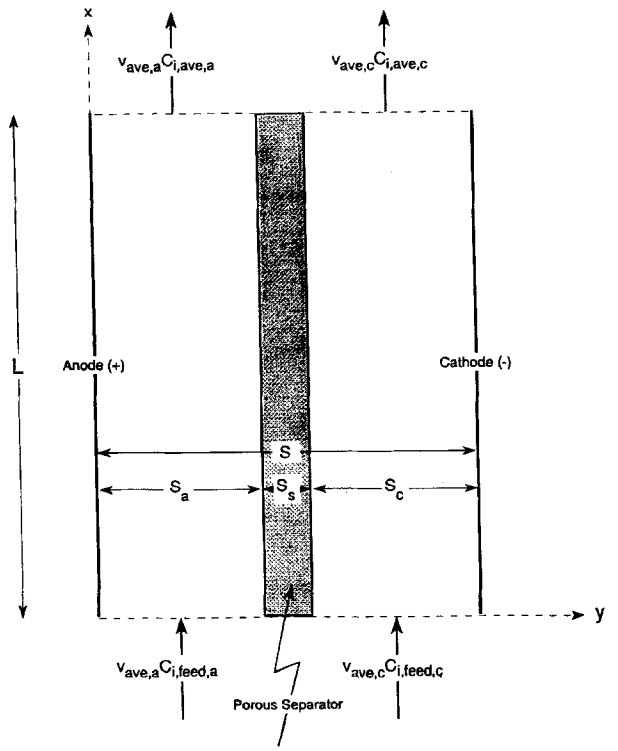

Fig. 1. Schematic diagram of a divided cell parallel-plate electrochemical reactor.

Model Development

In a caustic solution at a lead or nickel electrode, the important cathodic reactions involving nitrogenous species are believed to be[1]

$$\frac{1}{2}NO^-_{3(aq)} + \frac{1}{2}H_2O_{(l)} + e^- \rightleftarrows \frac{1}{2}NO^-_{2(aq)} + OH^-_{(aq)} \qquad U^{\theta 14,15} = 0.01 \quad [1]$$

$$\frac{1}{6}NO^-_{2(aq)} + \frac{5}{6}H_2O_{(l)} + e^- \rightleftarrows \frac{1}{6}NH_{3(g)} + \frac{7}{6}OH^-_{(aq)} \qquad -0.165 \quad [2]$$

$$\frac{1}{3}NO^-_{2(aq)} + \frac{2}{3}H_2O_{(l)} + e^- \rightleftarrows \frac{1}{6}N_{2(g)} + \frac{4}{3}OH^-_{(aq)} \qquad 0.406 \quad [3]$$

$$\frac{1}{2}NO^-_{2(aq)} + \frac{3}{4}H_2O_{(l)} + e^- \rightleftarrows \frac{1}{4}N_2O_{(g)} + \frac{3}{2}OH^-_{(aq)} \qquad 0.15 \quad [4]$$

$$H_2O_{(l)} + e^- \rightleftarrows \frac{1}{2}H_{2(g)} + OH^-_{(aq)} \qquad -0.828 \quad [5]$$

The reactions at the anode are

$$OH^-_{(aq)} \rightleftarrows \frac{1}{4}O_{2(g)} + \frac{1}{2}H_2O_{(l)} + e^- \qquad U^{\theta 14,15} = 0.401 \quad [6]$$

$$\frac{1}{2}NO^-_{2(aq)} + OH^-_{(aq)} \rightleftarrows \frac{1}{2}NO^-_{3(aq)} + \frac{1}{2}H_2O_{(l)} + e^- \qquad 0.01 \quad [7]$$

Reactions 5 and 7 are undesirable reactions that should be minimized by optimizing the design and operating conditions for the electrochemical reactor.

A porous separator is included in the model to reduce the oxidation of nitrite at the anode (reaction 7) and to keep the product gases of each electrode separate. It is thought to be important to separate the oxygen produced at the anode from the ammonia and any other potentially explosive gases which are produced at the cathode. A schematic diagram of a divided cell parallel-plate reactor is shown in Fig. 1. In the divided cell, a separator divides the anolyte and catholyte channels. The waste solution flows through the catholyte side of the cell, and a caustic solution flows through the anolyte channel.

Since the true reaction pathways for reactions 1-7 above are not known, it was assumed in this research that the kinetics of the model could be described by these equations. The reactions listed above (Eq. 1-7) also form a complete set of reactions from a stoichiometric viewpoint.[16]

Electrochemical reactor model assumptions.—The assumptions for the electrochemical reactor model are:

1. Steady state is achieved.
2. No homogeneous reactions occur (*i.e.*, the only reactions are those that occur at the electrodes).
3. The physical transport parameters are constant.
4. Dilute solution theory[17] applies.
5. The Nernst-Einstein equation,[17] $u_i = D_i/RT$, applies.
6. The Butler-Volmer equation can be used to describe the reactions at the electrodes.
7. The fluid is an incompressible Newtonian fluid in well-developed laminar flow. This assumption seems reasonable if the fluid is under high pressure, or if the flow rates are much higher than the gas evolution rates.[8]
8. Isothermal conditions exist.
9. The gases that are produced at the electrodes stay in solution in the reactor and are flashed after passing through the reactor.

In addition, it is assumed in this research that the relative activity of an ionic species can be approximated by the concentration of the ionic species and that the activity of a gaseous species can be approximated by the partial pressure of the species.

The equation development for the model is written in a general manner for a generic species i. In the model the species i includes ions and gases in solution. Some of the equations used in the model have been developed previously.[3-5,7] The equations for the reactor portion of the model are summarized in Tables I and II in this work, but are shown in detail in another work.[18]

In this study the change in concentration in the axial direction, $\partial C_i(x, y)/\partial x$ (or $\partial\theta_i/\partial\zeta$ in dimensionless variables),

Table I. Governing equations.

Anolyte/catholyte flow channels:		$-\left(\frac{\partial^2\theta_i}{\partial\xi^2}\right)$	[38]
	Mass continuity equation	$-z_i\left(\theta_i\frac{\partial^2\Phi}{\partial\xi^2}+\frac{\partial\theta_i}{\partial\xi}\frac{\partial\Phi}{\partial\xi}\right)$ $+3Pe\alpha\delta_i\frac{\partial\theta_i}{\partial\zeta}(\xi'-\xi'^2)=0$	
	Electroneutrality	$\sum_i z_i\theta_i C_{i,ref}=0$	[39]
Separator region:			
	Mass continuity equation	$-\left(\frac{\partial^2\theta_i}{\partial\xi^2}\right)$ $-z_i\left(\theta_i\frac{\partial^2\Phi}{\partial\xi^2}+\frac{\partial\theta_i}{\partial\xi}\frac{\partial\Phi}{\partial\xi}\right)=0$	[40]
	Electroneutrality	$\sum_i z_i\theta_i C_{i,ref}=0$	[41]

Table II. Boundary conditions.

Anode:			
	Electrochemical reactions	$\sum_j \frac{s_{ij} i_{j,n}}{n_j F} = -N_{i,n}$	[42]
	Electroneutrality	$\sum_i z_i \theta_i C_{i,ref} = 0$	[43]
Anolyte/separator interface:	Continuity of flux	$\left(\frac{\partial \theta_i}{\partial \xi} + z_i \theta_i \frac{\partial \Phi}{\partial \xi}\right) = \frac{1}{N_M}\left(\frac{\partial \theta_i}{\partial \xi} + z_i \theta_i \frac{\partial \Phi}{\partial \xi}\right)$ Anolyte side Separator side	[44]
	Electroneutrality	$\sum_i z_i \theta_i C_{i,ref} = 0$	[45]
Separator/catholyte interface:	Continity of flux	$\left(\frac{\partial \theta_i}{\partial \xi} + z_i \theta_i \frac{\partial \Phi}{\partial \xi}\right) = \frac{1}{N_M}\left(\frac{\partial \theta_i}{\partial \xi} + z_i \theta_i \frac{\partial \Phi}{\partial \xi}\right)$ Catholyte side Separator side	[46]
	Electroneutrality	$\sum_i z_i \theta_i C_{i,ref} = 0$	[47]
Cathode:			
	Electrochemical reactions	$\sum_j \frac{s_{ij} i_{j,n}}{n_j F} = N_{i,n}$	[48]
	Electroneutrality	$\sum_i z_i \theta_i C_{i,ref} = 0$	[49]

is treated as a time-like derivative and is approximated by taking small step sizes down the reactor length. The derivative is approximated as

$$\frac{\partial C_i(x, y)}{\partial x} \approx \frac{C_i(x + \Delta x, y) - C_i(x, y)}{L} \quad [8]$$

Instead of taking multiple steps down the reactor length a one-step[4] approximation is used for approximating the change in concentration in the axial direction. The change in concentration in the axial direction is approximated as $\partial C_i(x, y)/\partial x \approx C_i(x = L, y) - C_i(x = 0, y)/L$. This method has been shown previously to be a justified approximation if the conversion per pass in the reactor is not high.[4,5,7]

In dimensionless variables, the one-step approximation becomes

$$\frac{\partial \theta_i}{\partial \zeta} \approx \frac{\theta_i(\zeta = 1) - \theta_i(\zeta = 0)}{1} = \theta_i(\zeta = 1) - \theta_{i,feed} \quad [9]$$

Using this one-step approach essentially changes the model equations from two-dimensional to one-dimensional, thus a significant savings in computing time results. The $\theta_{i,feed}$ are known inlet conditions (initial conditions), and the θ_i that are solved for are the outlet dimensionless concentrations as functions of the lateral positions (v or ξ).

The current density which appears in the boundary condition is assumed to be given by the Butler-Volmer equation

$$i_{j,n} = i_{oj,ref}\left\{\prod_i \left(\frac{C_{i,o}}{C_{i,ref}}\right)^{p_{ij}} \exp\left[\alpha_{aj} f \eta_j\right] - \prod_i \left(\frac{C_{i,o}}{C_{i,ref}}\right)^{q_{ij}} \exp\left[-\alpha_{cj} f \eta_j\right]\right\} \quad [10]$$

where

$$\eta_j = V - \phi_o - U_{j,ref} \quad [11]$$

$$f = \frac{F}{RT} \quad [12]$$

In dimensionless variables the Butler-Volmer equation becomes

$$i_{j,n} = i_{oj,ref}\left\{\prod_i \theta_i^{p_{ij}} \exp\left[\alpha_{aj} f \eta_j\right] - \prod_i \theta_i^{q_{ij}} \exp\left[-\alpha_{cj} f \eta_j\right]\right\} \quad [13]$$

The initial conditions are just the specified feed conditions into the reactor (*i.e.*, all of the $\theta_{i,feed}$ are specified).

Modeling of an Electrochemical Reactor with a Recirculation Tank

In practice it is desirable to destroy 95% of the nitrate and nitrite species present in liquid radioactive waste before permanent disposal of the waste.[1] Since previous experimental work[2] and the models developed here indicate that the conversion per pass $[C_{i,ave}(x = 0) - C_{i,ave}(x = L)/C_{i,ave}(x = 0)]$ for nitrate reduction in a parallel-plate electrochemical reactor is very small, recirculation of the feed is needed to achieve an overall conversion of 95%. Another alternative would be to build a very long reactor; however, this is probably not feasible because of the high rate of gas evolution. The gases produced in the reactor increase the ohmic resistance of the cell. In a long reactor these gases would need to be released from the reactor to avoid large power losses. Some optimum combination of recycling and reactor length needs to be found.

A recirculation tank was included in this work to model the time dependent concentration of species in an alkaline nitrate/nitrite solution. A divided cell parallel-plate electrochemical reactor with two recirculation tanks (one for anolyte, one for catholyte) is shown in Fig. 2.

PPER with recirculation tank model equation development.—It is assumed in the model that the gases produced according to reactions 2-6 stay in solution inside the electrochemical reactor. After passing through the reactor, a flash occurs (either prior to or in the reservoir).

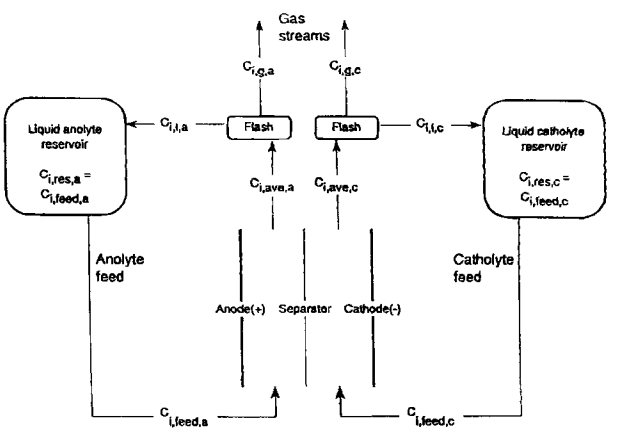

Fig. 2. Schematic diagram showing flash process for a divided cell parallel-plate reactor with recirculation tanks.

It is also assumed in this study that the reactor operates at steady state and that the only time dependence is in the recirculation tank. The following further assumptions were used for modeling the system:

1. The liquid in the reservoir (recirculation tank) is perfectly mixed, and there is no dead time between the reservoir and the reactor. Thus, $C_{i,res} = C_{i,feed}$.
2. The volumetric flow rate into the reservoir equals the volumetric flow rate out of the reservoir.
3. There is constant density of the liquid phase in the reservoir.
4. Henry's law holds for O_2, N_2, N_2O, H_2.
5. Raoult/s law can be used for H_2O, NH_3.

The equilibrium expressions needed are K_i values. In general, these are dependent upon pressure, temperature, and the composition in each phase. If Raoult's and Henry's laws are assumed to hold, the K_i values are functions of only the pressure and temperature of the system. The K_i value using Henry's law is of the form

$$K_i = \frac{y_i}{x_i} = \frac{H_{i,B}(T)}{P} \quad [14]$$

The value for Henry's constant, $H_{i,B}$, for a given species i is dependent upon the temperature and the solvent B. In this study the Henry's constants used were those for the gases in water at 298.15 K.

The K_i value, assuming Raoult's law, is of the form

$$K_i = \frac{y_i}{x_i} = \frac{P_i^{sat}(T)}{P} \quad [15]$$

The saturation pressure values in this study were calculated by using Antoine's equation.

The data needed for a flash calculation is the overall mole fraction of each species, z_i, the temperature and pressure of the system, and vapor-liquid equilibrium expressions for each species. Note that the z_i are independent of the pre-equilibrium phases that may be present. In general

$$z_i = x_i L + y_i V \quad [16]$$

where x_i is the mole fraction of species i in the liquid phase, y_i is the gas-phase mole fraction of species i, and L and V are the total mole fractions in the liquid and gas phase, respectively.

Prior to doing a flash calculation, it is important to first insure that the system is in the two-phase region. Thus dew point and bubble point calculations must also be done. Since the temperature and pressure are constant in this model, either dew point pressure and bubble point pressure or dew point temperature and bubble point temperature calculations can be done. Since the pressure is easier to solve for in these calculations, dew point pressure and bubble point pressure calculations were done prior to the flash calculation. The governing equations for the flash calculations are shown below.

The flash criteria used in this study are

$$\sum_i x_i = 1 \quad [17]$$

$$\sum_i y_i = 1 \quad [18]$$

$$L + V = 1 \quad [19]$$

$$\sum_i z_i = \sum_i (x_i L + y_i V) = 1 \quad [20]$$

From these criteria, the following flash equation (a function of vapor fraction) can be found[19]

$$f_{Flash}(V) = \sum_i \frac{z_i(K_i - 1)}{1 + V(K_i - 1)} = 0 \quad [21]$$

and

$$\frac{df_{Flash}}{dV} = -\sum_i \frac{z_i(K_i - 1)^2}{[1 + V(K_i - 1)]^2} \quad [22]$$

The value of V is the only unknown in the flash equation. Initially, this value must be guessed with the constraint that $0 < V < 1$. Successive estimates of V are found by

$$V_{k+1} = V_k - \left(\frac{f_{Flash}}{\frac{df_{Flash}}{dV}}\right)_k \quad [23]$$

After solving for the vapor mole fraction, V, the liquid and gas-phase mole fractions are found by

$$x_i = \frac{z_i}{L + K_i(1 - L)} \quad [24]$$

$$y_i = \frac{z_i - x_i L}{V} \quad [25]$$

The bubble point calculation is done to check to see if the system is in the two-phase region. This is necessary before doing a flash calculation because meaningless or incorrect results from the flash calculation will occur if the flash calculation is carried out and the system is not in the two-phase region. For a bubble point calculation, all of the components are assumed to be in the liquid phase, thus $z_i = x_i$. The temperature is constant in this work, and we are calculating the bubble point pressure.

The bubble point criterion is

$$\sum_i y_i = \sum_i K_i x_i = 1 \quad [26]$$

Multiplying through by the total pressure we get

$$\sum_i K_i P x_i = P \quad [27]$$

or

$$f_{BublP}(P) = P - \sum_i K_i P x_i = 0 \quad [28]$$

Since the K_i values have pressure in the denominator, the second term in the bubble point equation has no net pressure term and

$$\frac{df_{BublP}}{dP} = 1.0 \quad [29]$$

Iterative estimates of the bubble point pressure can be done using Newton's method

$$P_{k+1} = P_k - \left(\frac{f_{BublP}}{\frac{df_{BublP}}{dP}}\right)_k = P_k - \left(\frac{f_{BublP}}{1.0}\right)_k \quad [30]$$

until convergence is reached.

In a dew point calculation, all of the species are assumed to be in the gas phase. Thus, $y_i = z_i$. In this research the K_i values for the ions are taken to be zero, and thus there is no possible gas only phase. Nevertheless, the dew point calculation was programmed (equations shown elsewhere[16]) to keep the program general and allow use with other K_i values.

The gases produced electrochemically in the reactor are assumed to stay in solution in the reactor and are flashed after leaving the reactor but before the reservoir. A gas phase and liquid phase then exist and are split from one another. The liquid phase then goes into the recirculation tank. The tank is perfectly mixed, and the exit from the tank is the feed to the electrochemical reactor. Figure 2 shows a schematic diagram of this arrangement.

The z_i values in this case are the x_i values from the outlet of the reactor since all of the gases are assumed to be in solution at this point. Thus

$$z_i = \frac{C_{i,ave} v_{ave}}{\sum_i C_{i,ave} v_{ave}} \quad [31]$$

for a flash calculation that occurs just after the reactor.

Table III. Base case kinetic parameters

Reaction j	$i_{o,j,ref}$ (A/cm^2)	$\alpha_{a,j}$	$\alpha_{c,j}$	n_j	U_j^{θ} [14,15] (V *vs.* SHE)	$U_{j,ref}$ (V *vs.* SHE)
1	8.0e − 10	0.5	0.5	1	0.01	0.0178
2	8.5e − 11	0.5	0.5	1	−0.165	−0.1388
3	3.0e − 15	0.5	0.5	1	0.406	0.390
4	1.5e − 13	0.5	0.5	1	0.15	0.1514
5	3.0e − 06	0.5	0.5	1	−0.828	−0.8384
6	1.9e − 11	0.5	0.5	1	0.401	0.3920
7	1.0e − 15	0.5	0.5	1	0.01	0.0178

The governing equation for the recirculation tank is then the same as that for a recirculation tank for a system with no gases being evolved. Thus

$$\frac{d(C_{i,res}V_{res})}{dt} = \mathcal{V}_l C_{i,l} - \mathcal{V}_{feed} C_{i,feed} \quad [32]$$

where $C_{i,l}$ is the liquid-phase concentration of species i resulting from the flash calculation, as can be seen in Fig. 2. $\mathcal{V}_l$ is the volumetric flow rate of this stream. In this work, it was assumed that this flow rate is the same as the flow rate for the feed to the reactor, $\mathcal{V}_{feed}$. Thus $\mathcal{V}_{feed} = \mathcal{V}_l$ = a constant.

The time derivative was approximated by a step change in time

$$\frac{dC_{i,res}}{dt} \approx \frac{C_{i,res}(t + \Delta t) - C_{i,res}(t)}{\Delta t} \quad [33]$$

Since the reactor is perfectly mixed, $C_{i,res} = C_{i,feed}$, and the governing equation for the reservoir becomes

$$C_{i,feed}(t + \Delta t) = C_{i,feed}(t) + \Delta t \frac{\mathcal{V}_{feed}}{V_{res}} [C_{i,l}(t) - C_{i,feed}(t)] \quad [34]$$

Model Parameters

The physical and operating parameters are shown in Table III. The flow rates, cell dimensions, and other parameters, were chosen based upon previous and planned experimental work by others.[2] These values were used in the case studies presented here, unless otherwise stated.

The base case values of species-specific parameters used in this work appear in Table IV. The diffusion coefficients used for the ionic species are from limiting ionic conductivity data.[17] The diffusion coefficients for the gases were estimated from the Wilke-Chang estimation method, assuming the water is the solvent.[20] The values for initial feed concentrations, $C_{i,feed}$, used are similar to those used in previous and planned experimental work.[1,2]

The base case kinetic parameters used in this study are shown in Table V. The values are the same for both the undivided and divided cells. The values for the exchange current densities were guessed after setting all the other model parameters to obtain results similar to experimental data.[2]

The following reaction orders were used in this study

$$\text{If } s_{i,j} > 0, \text{ then } p_{i,j} = s_{i,j},\ q_{i,j} = 0$$

$$\text{If } s_{i,j} < 0, \text{ then } p_{i,j} = 0,\ q_{i,j} = -s_{i,j}$$

Table VI shows a list of the equilibrium K_i values used in this study for the flash calculations.

Table IV. Base case physical and operating parameters.

$\mathbf{v}_{ave,a}$	10.50 cm/s
$\mathbf{v}_{ave,c}$	10.50 cm/s
W (electrode breadth)	10.00 cm
L (electrode length)	10.00 cm
S_a (anolyte width)	0.60 cm
S_c (catholyte width)	0.60 cm
S_s (separator width)	0.05 cm
S (electrode gap)	1.25 cm
MacMullin number	5.00
Temperature	298.15 K
Anolyte volume	7000.00 ml
Catholyte volume	700.00 ml

Solution Procedure

The parallel-plate reactor model governing equations results in a set of coupled differential and algebraic equations. A finite-difference approximation method was used for the derivatives. This resulted in a system of coupled algebraic equations. These equations were then solved using a Newton-Raphson-type procedure developed by Newman called Band(J).[17] A modified form of the procedure, mband,[21] was used to allow multiple regions to be modeled.

The solution steps used for the reactor and reservoir models together are:

1. Solve the parallel-plate reactor model using initial conditions (base case feed conditions in Table V). This is time $t = 0$.
2. Use the average outlet concentration at time t and the flow rate of the solution(s) to solve the bubble point, dew point, and flash calculations. Then solve for the liquid composition going into the reservoir.
3. Calculate the new reservoir concentration at time $t + \Delta t$ using Eq. 34. This is the new feed to the reactor.
4. Solve for the new outlet concentrations from the reactor and then return to step 2.
5. Repeat steps 2-4 until some specified time or charge has been passed.

The case studies presented in this work were run until one million coulombs had passed to compare the results with some previous experimental work where this was done.[2]

Material balance closure calculations were also programmed for the electrochemical reactor in the same way as has previously been done by others.[4] The results verified the consistency of the model from a material balance perspective.

Results and Discussion

In evaluating the effectiveness of the destruction process, determining the current efficiency for each reaction is important. The current efficiency for a reaction j, ϵ_j, is defined as

$$\epsilon_j = \frac{i_j}{i_{tot}} = \frac{i_j}{\sum_k i_k} \quad [35]$$

Since the current density for a reaction is directly related to the rate of reaction through Faraday's law, the current efficiency gives a measure of the selectivity for each reaction.

It should be noted that

$$\sum_1^5 \epsilon_j = 1 \quad [36]$$

$$\sum_6^7 \epsilon_j = 1 \quad [37]$$

or that the sum of the current efficiencies at each electrode is one.

The parallel-plate reactor model was programmed to explicitly calculate the current density for each reaction (i_j appears in the electrode boundary conditions). Thus, current efficiency predictions can be made using the model.

In an operating parallel-plate reactor for the destruction of nitrate and nitrite waste, it is desirable to maximize the current efficiency (cathodic) of reactions 1-4 and minimize

Table V. Base case species parameters.

Species i	z_i	D_i [a] (cm^2/s)	$C_{i,ref}$ (mol/cm^3)	$C_{i,feed}$ (mol/cm^3)	$\theta_{i,feed,a}$	$\theta_{i,feed,c}$
$NO_{3(aq)}^-$	−1	1.902e − 05	1.95e − 3	1.95e − 3	1.0e − 4	1.0
$NO_{2(aq)}^-$	−1	1.902e − 05	0.60e − 3	0.60e − 3	1.0e − 4	1.0
$OH_{(aq)}^-$	−1	5.260e − 05	1.33e − 3	1.33e − 3	2.917	1.0
$Na_{(aq)}^+$	1	1.334e − 05	3.88e − 3	3.88e − 3	1.0	1.0
$N_{2(aq)}$	0	1.900e − 05	1.0e − 06	1.0e − 10	1.0e − 4	1.0e − 4
$NH_{3(aq)}$	0	2.168e − 05	1.0e − 06	1.0e − 10	1.0e − 4	1.0e − 4
$N_2O_{(aq)}$	0	1.801e − 05	1.0e − 06	1.0e − 10	1.0e − 4	1.0e − 4
$O_{2(aq)}$	0	2.151e − 05	1.0e − 06	1.0e − 10	1.0e − 4	1.0e − 4
$H_{2(aq)}$	0	2.322e − 05	1.0e − 06	1.0e − 10	1.0e − 4	1.0e − 4

[a] Ionic species diffusion coefficients from limiting conductivity data.[17] Nonionic species diffusion coefficients estimated using the Wilke-Chang estimation method.[20]

the current efficiency of reaction 5 (the production of hydrogen). At the anode, it is desirable to maximize the current efficiency of reaction 6 (oxidation of hydroxide) and to minimize the current efficiency of reaction 7 (oxidation of nitrite to nitrate).

Figures 3-8 show the results from a case study with the base-case parameters and E_{cell} = 3.5 V. In this case the catholyte reservoir volume used is 700 ml, and the anolyte reservoir volume is 7000 ml. A large anolyte reservoir volume is used so that the depletion of $OH_{(aq)}^-$ in the anolyte will not be large, which would cause limitations in the current density later in the run.

Figure 3 shows the cathodic current efficiencies *vs.* coulombs passed. Initially the current efficiency is greatest for the nitrate reduction reaction (reaction 1), but the nitrite to ammonia reaction current efficiency (reaction 2) soon becomes large as the concentration of nitrite increases. Nitrite to nitrogen and nitrite to nitrous oxide reaction current efficiencies also increase but not to as large an extent (reactions 3 and 4, respectively).

The oxidation of nitrite to nitrate (reaction 7) does not consume much of the current in the divided cell, as can be seen in Fig. 4. The current efficiency for this reaction is extremely small at the beginning of the run (<0.01%). As nitrite diffuses and migrates through the separator, this current density increases but never becomes large. The maximum current efficiency reached is about 1.3% and levels off at this value as the concentration of nitrite in the catholyte is low by this time. Thus there is no net driving force moving the nitrite from the catholyte to the anolyte. Migration tends to move the nitrite and nitrate into the anolyte from the catholyte, but when the concentration in the catholyte becomes small enough, the migration and diffusion cancel each other.

The concentration of ionic species in the catholyte reservoir *vs.* coulombs passed is shown in Fig. 5. The concentration of $Na_{(aq)}^+$ increases as the run proceeds due to migration from the anolyte. While electroneutrality must always be maintained and $OH_{(aq)}^-$ is being produced at the cathode, the amount of $Na_{(aq)}^+$ that is transported into the catholyte is dependent upon the volume of the anolyte reservoir. Migration tends to move the sodium ions toward the catholyte; diffusion tends to move the sodium back toward the anolyte. This diffusion term would be even more important if the concentration of $Na_{(aq)}^+$ dropped substantially in the anolyte (due to movement into the catholyte). With a large anolyte reservoir, however, this is not the case, as can be seen in Fig. 6.

The concentrations of nitrate and nitrite drop rapidly in the catholyte reservoir because the reduction of nitrate to nitrite is not reversed at the anode. This can be seen in Fig. 5. The concentration of $NO_{3(aq)}^-$ and $NO_{2(aq)}^-$ drop to approximately 1 and 5% of their original concentrations, respectively, after one million coulombs have passed.

Figure 6 shows that the concentrations of nitrate and nitrite in the anolyte do increase as the run continues due to diffusion and migration from the catholyte, but the concentrations never become very high (<0.06*M* each after one million coulombs have passed). When these species are consumed at the cathode, the concentration in the catholyte drops, thus decreasing the tendency for ions to diffuse into the anolyte. The mass transport of these ions could be decreased further by increasing the effective separator thickness ($N_M S_s$) of the separator or by using an ion exchange membrane such as Nafion®.

Several interesting phenomena are observed in the catholyte and anolyte off-gases. The catholyte off-gas composition *vs.* coulombs passed for this case of the divided cell is shown in Fig. 7. The flash calculation initially predicts that there is no gas phase until the concentration of the gases in solution increases. Thus in Fig. 7, the compositions initially all start at zero and then jump up after a small amount of charge has been passed. Nitrogen and nitrous oxide are the major gases at the beginning of the run, even

Table VI. Gas species equilibrium K_i values used in this study.

Gas species i	H_i [24] or P_i^{sat} [25] (298.15 K)	K_i (2.98.15 K)
N_2	H = 8.56e04 atm	8.56e04
N_2O	H = 3.0e03 atm[a]	3.0e03
O_2	H = 4.34e04 atm	4.34e04
H_2	H = 7.03e04 atm	7.03e04
NH_3	P^{sat} = 9.98 atm	9.98
H_2O	P^{sat} = 0.03 atm	0.03

[a] Estimated value.

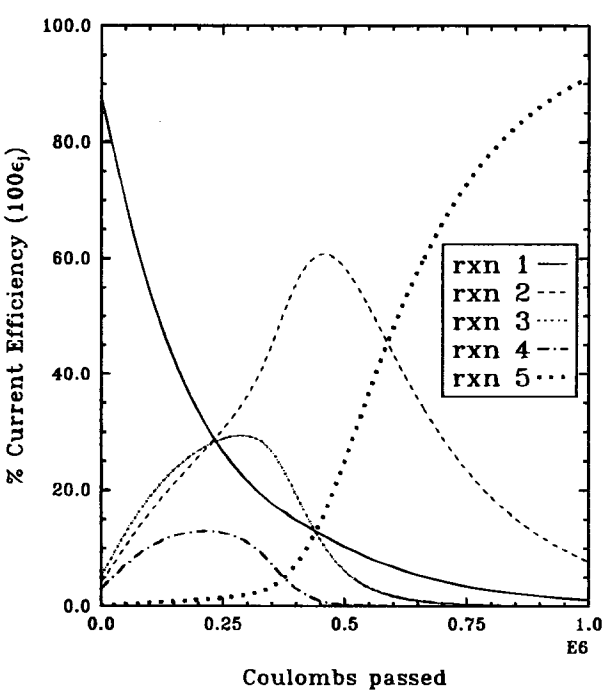

Fig. 3. Divided cell cathodic current efficiencies *vs.* coulombs passed when E_{cell} = 3.5 V.

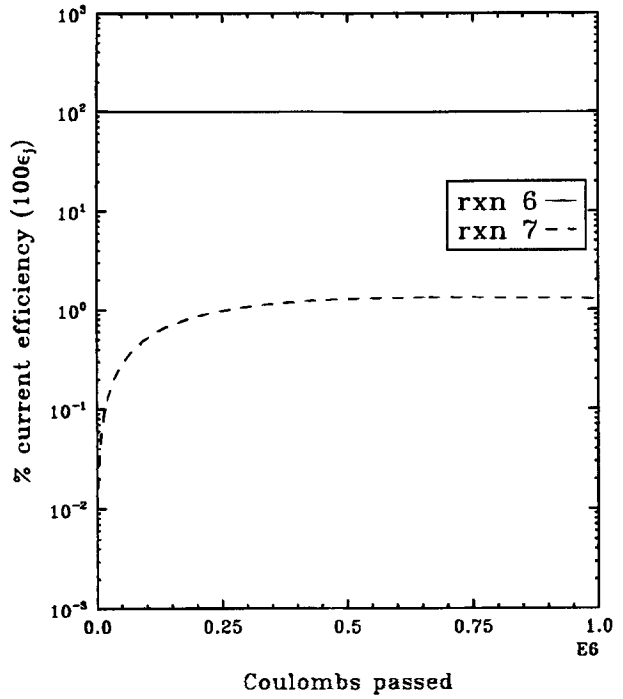

Fig. 4. Divided cell anodic current efficiencies *vs.* coulombs passed when E_{cell} = 3.5 V.

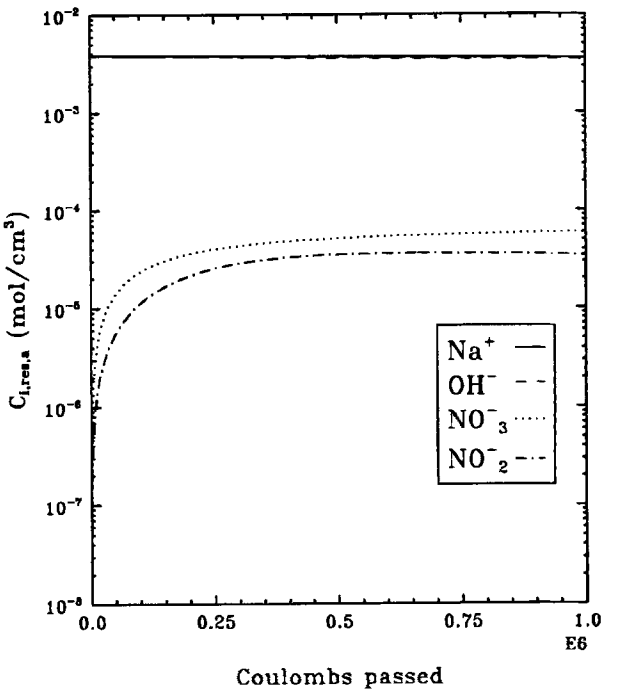

Fig. 6. Divided cell anolyte reservoir ionic concentrations *vs.* coulombs passed when E_{cell} = 3.5 V.

though the current efficiency for the nitrous oxide reaction (reaction 4) is low compared to the reaction producing ammonia (reaction 2). This is because the solubility of ammonia is much higher than that for the nitrogen and nitrous oxide. Hydrogen gas is initially the third largest component of the off-gas, even though the current efficiency for this reaction is very small initially. Again, this is because the solubility of hydrogen is very small; essentially any hydrogen that is produced goes into the gas phase. Later in the run the hydrogen gas becomes the major off-gas when the current efficiency for this reaction increases after most of the nitrate and nitrite have been consumed.

The concentration of ammonia in the off-gas increases during the first half of the run but slowly decreases during the second half when the nitrite is consumed and the current efficiency for this reaction (reaction 2) decreases. The off-gas ammonia composition is seen to be smaller than the other cathodically produced gases even though the majority of gas-producing current goes through this reaction. This is due to the solubility of the ammonia being greater than that for the other gases. In this case study, the equilibrium K_i value for ammonia is assumed to be given by Raoult's law. In a pure water/ammonia system, the solubility of the ammonia is even greater than predicted by Raoult's law.[22] In a caustic solution, however, the solubility

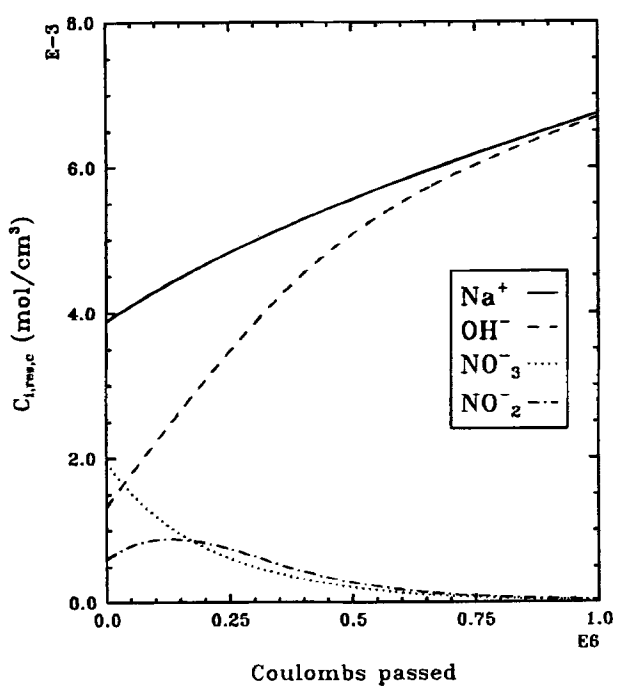

Fig. 5. Divided cell catholite reservoir ionic concentrations *vs.* coulombs passed when E_{cell} = 3.5 V.

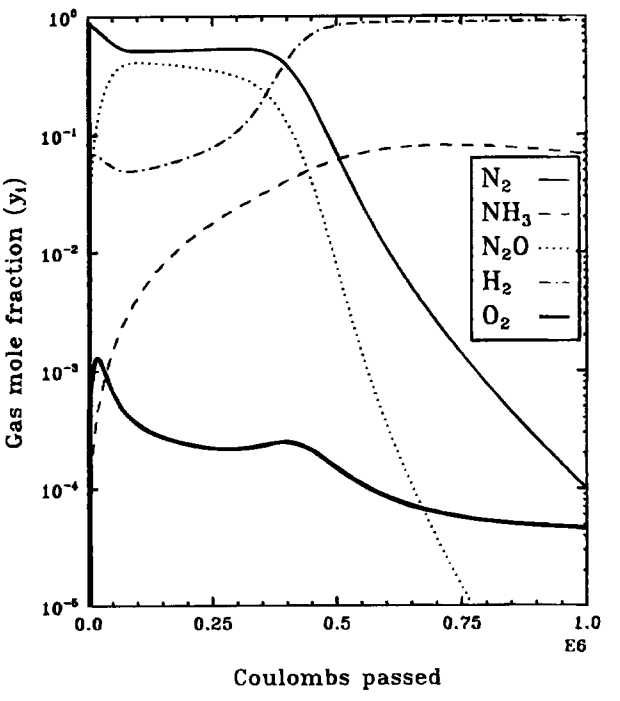

Fig. 7. Divided cell catholyte off-gas composition (mole fraction) *vs.* coulombs passed when E_{cell} = 3.5 V.

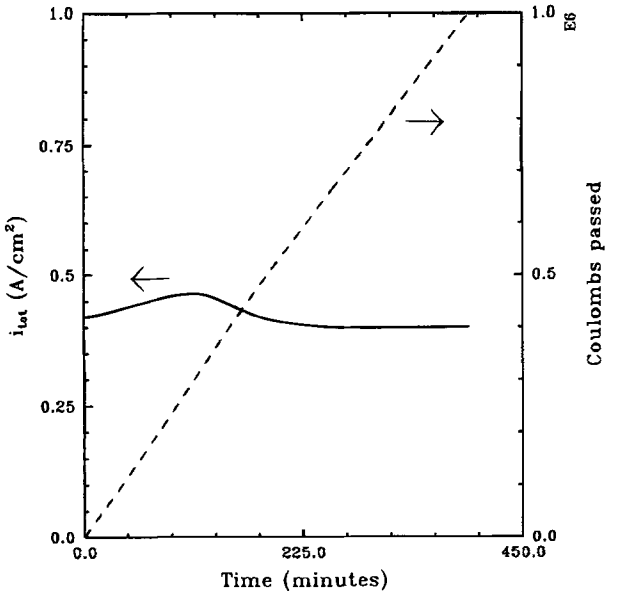

Fig. 8. Divided cell current density and coulombs passed *vs.* time when E_{cell} = 3.5 V.

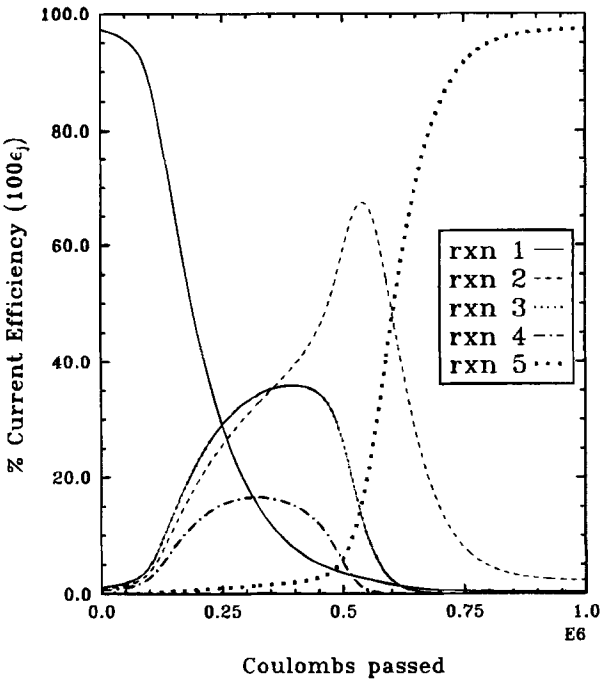

Fig. 9. Divided cell cathodic current efficiencies *vs.* coulombs passed when E_{cell} = 3.0 V.

is less than that for a water/ammonia system.[1] In addition, the solubility of the ammonia will decrease if the temperature of the system is increased. Thus if the temperature of the system increases during the reaction, as has been found in some experimental work by others,[2,23] more of the ammonia in solution will move into the gas phase and may continue to move into the gas phase even if the production rate at the cathode decreases. An increase in temperature will not affect the amount of the other gases in the off-gas as much as ammonia because the solubilities of the other gases are very low already. Thus there is not as much of these species present in the aqueous phase to be released if the temperature increases.

The concentration of oxygen in the catholyte off-gas is small throughout the run because the only source of oxygen is from anodically produced oxygen that diffuses through the separator. The mole fraction of oxygen decreases throughout the run as the total amount of the other gases increases due to the occurrence of higher rates of the gas producing cathodic reactions, especially the hydrogen evolution reaction.

Figure 8 shows the current density and coulombs passed *vs.* time for the divided cell. The current density rises a small amount initially but then drops when the nitrate and nitrite catholyte concentration drops.

The divided model was run again at a lower applied potential (E_{cell} = 3.0 V). The results from this case are shown in Fig. 9-12. The results are similar to the previous case, but there are some important differences. Figure 9 shows the catholyte current efficiencies *vs.* coulombs passed. The current efficiency of reaction 1 (nitrate to nitrite) is much higher at the beginning of the run than in the previous case (97% *vs.* 88% initially). As more coulombs are passed, the current efficiency for this reaction goes down, and the current efficiency for reactions 2-4 consuming nitrite go up. The destruction of nitrate and nitrite occurs with fewer coulombs passed because the current efficiency for these reactions is higher initially. The hydrogen evolution reaction does not occur until almost all of the nitrate and nitrite have been destroyed. Significant hydrogen evolution does not occur until more than 500,000 C have passed, whereas in the previous case, hydrogen evolution became significant at about 400,000 C. The catholyte nitrate and nitrite concentrations decreased after fewer coulombs were passed, as can be seen by comparing Fig. 10 (E_{cell} = 3.0 V) with Fig. 5 (E_{cell} = 3.5 V).

The catholyte off-gas composition is shown in Fig. 11. The results are similar in this case to those of the previous case (Fig. 7) in the second half of the run. The gases produced from the destruction of nitrite decrease further than in the previous case. This makes sense since there is not as much nitrite available to be reduced by this point.

The current density and coulombs passed in this run are shown in Fig. 12. The initial current density is much less initially in this run and drops to less than one-third of the current density of the previous run at 3.5 V during most run time. More than 1100 min are required to pass one million coulombs *vs.* 400 min for the run at 3.5 V. While taking a much longer time to pass a given amount of current, that same current is used more efficiently to destroy nitrate and nitrite. The energy consumed at 3.5 V is 16.7% higher than that at 3.0 V for the same amount of charge passed. Power

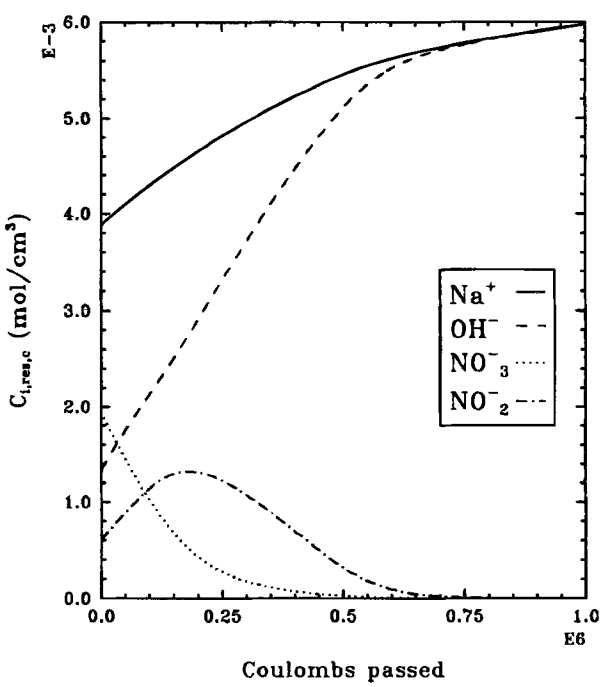

Fig. 10. Divided cell catholyte reservoir ionic concentrations *vs.* coulombs passed when E_{cell} = 3.0 V.

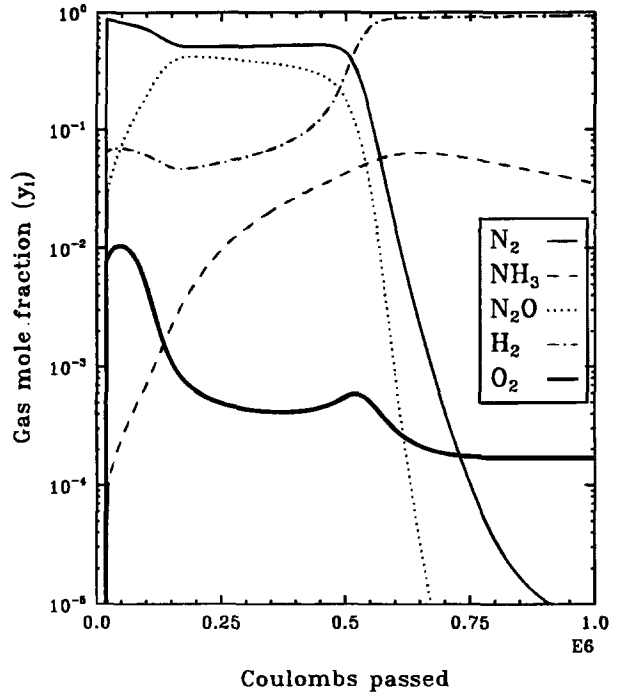

Fig. 11. Divided cell catholyte off-gas composition (mole fraction) *vs.* coulombs passed when E_{cell} = 3.0 V.

requirements are higher too, as both the current density and the voltage are higher in this case.

Conclusions

The case studies presented indicate that at lower applied potentials the destruction of nitrate and nitrate was carried out more effectively. Using a separator was effective in keeping the nitrite produced at the cathode from moving to the anode and being oxidized back to nitrate. If the destruction can be carried out at lower applied potentials, significant savings in energy and power requirements may be possible. The drawback to operating at lower potentials is that the time required for destroying the nitrate and nitrite species is increased. The savings in cost by operating at lower potential and current would need to be weighed against time constraints for destroying the waste.

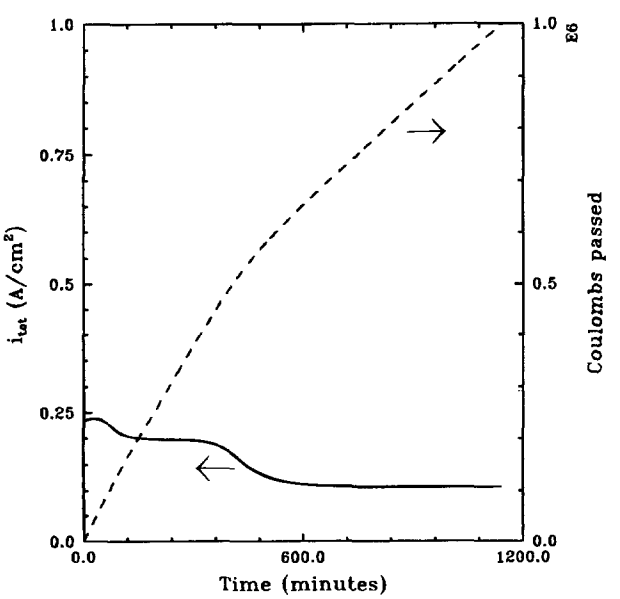

Fig. 12. Divided cell current density and coulombs passed *vs.* time when E_{cell} = 3.0 V.

Future work should include the comparison of model predictions with experimental data obtained from a reactor using the same operating conditions as used in the model. The data obtained from these experiments would be useful for optimizing the adjustable model parameters, such as exchange current densities, before further case studies are performed.

Acknowledgments

This work was funded by the Department of Energy Office of Technology Development, Office of Environmental Management through the Efficient Separations and Processing Integrated Program, Teresa B. Fryberger, Headquarters Program Manager, and James A. Wright, Cognizant Technical Program Officer.

Manuscript received July 25, 1994; revised manuscript received Nov. 15, 1994.

The University of South Carolina assisted in meeting the publication costs of this article.

LIST OF SYMBOLS

B	solvent in Henry's constant; assumed to be water in this study
C_i	concentration of species i, mol/cm^3
d_e	equivalent diameter, $2SW/S + W$, cm
D_i	diffusion coefficient of species i, cm^2/s
$D_{i,e}$	effective diffusion coefficient of species in the separator region, cm^2/s
f	function or governing equation (used for flash, bubble point, and dew point calculations)
F	Faraday's constant, 96,487 C/mol
$H_{i,B}$	Henry's constant for species i in solvent B
K_i	phase equilibrium value for species i, $K_i = y_i/x_i$
i_j	current density due to reaction j, A/cm^2
L	reactor length, cm
L	overall mole fraction in liquid phase
n_j	number of electrons passed in reaction j
$\mathbf{N}_i$	flux vector of species i, mol/(cm^2 s)
N_M	MacMullin number, $N_M = \tau/\epsilon = \rho/\rho_o$
N_i	flux of species i in the direction indicated, mol/(cm^2 s)
N_{Re}	Reynolds number, vd_e/ν
p_{ij}	anodic reaction order of species i in reaction j
P	total pressure, atm
P_i^{sat}	saturation pressure of species i, atm
q_{ij}	cathodic reaction order of species i in reaction j
R	gas law constant, 8.3143 J/(mol K)
R_i	rate of generation of species i due to homogeneous reaction, mol/s
s_{ij}	stoichiometric coefficient of species i in reaction j
S	distance between electrodes (electrode gap), cm
S_a	width of anolyte channel, cm
S_c	width of catholyte channel, cm
S_s	thickness of separator, cm
SHE	standard hydrogen electrode
t	time, s
T	temperature, K
u_i	mobility of species i, cm^2 mol/(J s)
U_j^θ	standard open-circuit potential of reaction j *vs.* SHE, V
$U_{j,ref}$	open-circuit potential of reaction j at reference conditions, V
$\mathbf{v}$	electrolyte velocity vector, cm/s
v	magnitude of electrolyte velocity, cm/s
V	electrote potential, V
V	overall mole fraction in the gas phase
$\mathcal{V}$	volumetric flow rate, cm^3/s
$\mathcal{V}_l$	volumetric flow rate of liquid stream into reservoir, cm^3/s
W	breadth of flow channel, cm
x	axial reactor position, cm
x_i	mole fraction of species i in the liquid phase
y	radial reactor position, cm
y_i	mole fraction of species i in the gas phase
z_i	charge number of species i
z_i	overall mole fraction of species i

Greek

α_{aj}	anodic transfer coefficient for reaction j
α_{cj}	cathodic transfer coefficient for reaction j
ϵ	porosity of the separator
ζ	dimensionless reactor axial distance, $\zeta = x/L$

η_j reaction overpotential at the electrode surface ($V - \Phi_o - U_{j,ref}$), V
θ_i dimensionless solution concentration, $\theta_i = C_i/C_{i,ref}$
ν kinematic viscosity of the electrolyte solution, cm^2/s
ξ dimensionless radial position, $\xi = y/S$
ξ' dimensionless distance between boundary conditions for the divided cell
ρ resistivity of the solution and separator together, Ω cm
ρ_o resistivity of the solution without a separator, Ω cm
τ tortuosity of the separator
ϕ solution potential, V
ϕ_o solution potential at the electrode/solution interface, V
Φ dimensionless solution potential, $\Phi = F/RT\ \phi$

Subscripts

a anolyte
ave average
BublP bubble point pressure
c catholyte
feed feed conditions to reactor
Flash refers to flash calculation
g gas
i species number
j reaction number
k iteration number; also used as an index of summation variable
ℓ liquid
n normal direction
o at the surface
r reference value
ref reference value or condition
res in the reservoir
s separator
tot total
x axial direction
y lateral direction

REFERENCES

1. D. T. Hobbs, in *Electrochemistry for a Cleaner Environment,* J. D. Genders and N. L. Weinberg, Editors, The Electrosynthesis Company, Amherst, NY (1992).
2. D. T. Hobbs, G. D. Genders, and D. Hartsough, Abstract 568, p. 910, The Electrochemical Society Extended Abstracts, Vol. 94-1, San Francisco, CA, May 22-27, 1994.
3. R. E. White, M. Bain, and M. Raible, *This Journal,* **130,** 1037 (1983).
4. M. J. Mader, C. W. Walton, and R. E. White, *ibid.,* **133,** 1124 (1986).
5. M. J. Mader and R. E. White, *ibid.,* **133,** 1297 (1986).
6. J. W. Van Zee, R. E. White, and A. T. Watson, *ibid.,* **133,** 501 (1986).
7. T. I. Evans and R. E. White, *ibid.,* **134,** 1866 (1987).
8. W. S. Wu, G. P. Rangaiah, and M. Fleischmann, *J. Appl. Electrochem.,* **23,** 113 (1993).
9. D. J. Pickett, *Electrochemical Reactor Design,* 2nd ed., Elsevier Scientific, New York (1979).
10. D. J. Pickett, *Electrochim. Acta,* **20,** 803 (1975).
11. A. T. S. Walker and A. A. Wragg, *ibid.,* **22,** 1129 (1977).
12. K. Scott and E. M. Paton, *ibid.,* **38,** 2181 (1993).
13. T. V. Nguyen, C. W. Walton, and R. E. White, *This Journal,* **133,** 1130 (1986).
14. A. J. Bard, R. Parsons, and J. Jordan, *Standard Potentials in Aqueous Solutions,* Marcel Dekker, Inc., New York (1985).
15. S. G. Bratsch, *J. Phys. Chem. Ref. Data,* **18** (1989).
16. D. H. Coleman, Master's Thesis, Texas A&M University, College Station, TX (1994).
17. J. S. Newman, *Electrochemical Systems,* 2nd ed., Prentice Hall, Englewood Cliffs, NJ (1991).
18. D. H. Coleman and R. E. White, in *Topics in Electrochemical Engineering: Proceedings of the Douglas N. Bennion Memorial Symposium,* J. Newman and R. E. White, Editors, PV 94-22, p. 374, The Electrochemical Society Proceedings Series, Pennington, NJ (1994).
19. J. M. Smith and H. C. Van Ness, *Introduction to Chemical Engineering Thermodynamics,* 4th ed., McGraw Hill, Inc., New York (1987).
20. R. C. Reid, J. M. Prausnitz, and B. E. Poling, *The Properties of Gases and Liquids,* 4th ed., McGraw Hill, Inc., New York (1987).
21. D. Fan, Ph.D. Thesis, Texas A&M University, College Station, TX (1991).
22. R. H. Perry and D. Green, *Perry's Chemical Engineers Handbook,* 6th ed., McGraw Hill, Inc., New York (1984).
23. D. Wingard, Personal communication, University of South Carolina, Columbia, South Carolina (1993).
24. P. W. Atkins, *Physical Chemistry,* 4th ed., Freeman and Company, Inc., New York (1990).
25. R. M. Felder and R. W. Rousseau, *Elementary Principles of Chemical Processes,* 2nd ed., Wiley, New York (1986).